INFLUENCE OF DC-ARC FURNACE GEOMETRY ON A 'COBALT FROM SLAG' PROCESS

R.T. Jones, T.G. la Grange, and G. Assis

Pyrometallurgy Division, Mintek, Private Bag X3015, Randburg, 2125, South Africa
E-mail: rtj@pyro.mintek.ac.za   glg@pyro.mintek.ac.za   ga@pyro.mintek.ac.za

ABSTRACT

Cobalt and other valuable metals can be recovered from a range of slags from non-ferrous smelters, using DC-arc furnace technology. This type of furnace offers sufficient process flexibility to ensure high recoveries of cobalt, nickel, copper, and any precious metals that may be present. The scale-up to industrial implementation of this process involves an understanding of the interrelationships between the chemical reactions, the mass transfer, the coalescence and settling of metal droplets, the electrical charactersitics, and the temperature distribution in the furnace. In this study, some of the effects of bath depth and width on the process are presented. The chemical composition of furnace products has been predicted and compared to the results of three experiments carried out at the same power levels and throughput, but using furnace shells of two different diameters operating off the same 200 kVA power supply.

Nickel – Cobalt 97
36th Annual Conference of Metallurgists, Sudbury, Canada, August 1997

Mintek Paper No. 8389

INTRODUCTION

In recent years, there has been a great deal of interest expressed in the recovery of valuable metals, such as cobalt and nickel, from a variety of slags. A process to carry this out, using a DC-arc furnace, has been under development since 1988 at Mintek, and has successfully been demonstrated at pilot scale (1). The process involves the selective carbothermic reduction of the oxides of cobalt, nickel, and copper, while retaining the maximum possible quantity of iron as oxide in the slag. Pilot-plant testwork at Mintek has demonstrated recoveries of 98% for nickel and over 80% for cobalt, at power levels of up to 600 kW. A DC-arc furnace offers sufficient process flexibility to ensure high recoveries of cobalt, nickel, copper, and any precious metals that may be present.

In the course of implementing this process industrially, it is necessary to establish how such a process can be scaled up. Among the most important parameters are those specifying the geometry of the furnace, i.e. the width and depth of the molten bath. It is widely understood that the width and depth of the furnace bath affect the power flux and energy distribution within the furnace, but it has not previously been shown what influence these geometric factors have on the chemistry of the process.

For a given feed rate of slag to be processed, the useful power requirement for the process can be calculated, using Pyrosim computer software (2), for example. These two variables (the feed rate and power) are the primary determinants of the overall size of the furnace. The third factor to consider is the residence time in the furnace, as previous work (1) has shown the influence of time on the residual level of cobalt in the slag. However, there remains a choice on the part of the furnace designer to select either a wide shallow bath, a narrow deep bath, or some combination of width and depth between these two extremes.

EXPERIMENTAL WORK

A series of tests was carried out to investigate the influence of bath depth and width, using two furnace shells of different diameters operating off the same 200 kVA power supply. These tests were carried out over a continuous period of three days, and involved the processing of about three and a half tons of slag.

Furnace configuration

The DC-arc furnace has been described elsewhere (1,3), but is essentially a refractory-lined cylindrical steel shell, having a single graphite electrode (cathode) positioned above the molten bath, and a multiple-pin anode located in the hearth. A schematic diagram of the furnace is shown in Figure 1.

Water-cooled electrode clamp
Water-cooled electrode seal
Off-gas port
Roof feed port
High-alumina cast water-cooled roof
Water-cooling jacket
Maximum slag level
Taphole
Chrome / magnesite refractory bricks
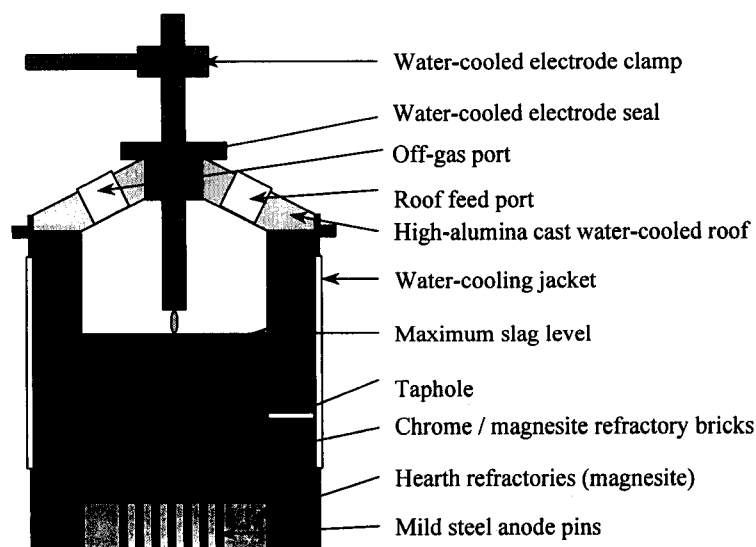Hearth refractories (magnesite)
Mild steel anode pins

Figure 1 – Schematic diagram of the DC-arc furnace

Two furnace shells, having internal diameters of 466 mm and 700 mm, were used for the tests. The smaller furnace had a single taphole, while the larger had two tapholes (so that two different bath depths could be tested). The furnaces are depicted in their full state, for all three conditions tested, in Figure 3. In each case, the material fed during each tap raises the level of the molten bath to a pre-defined maximum height. Once the complete batch has been fed, the furnace is drained to the level of the taphole. The fraction of molten material remaining below the taphole has an important bearing on the residence time of the material, as discussed in a later section.
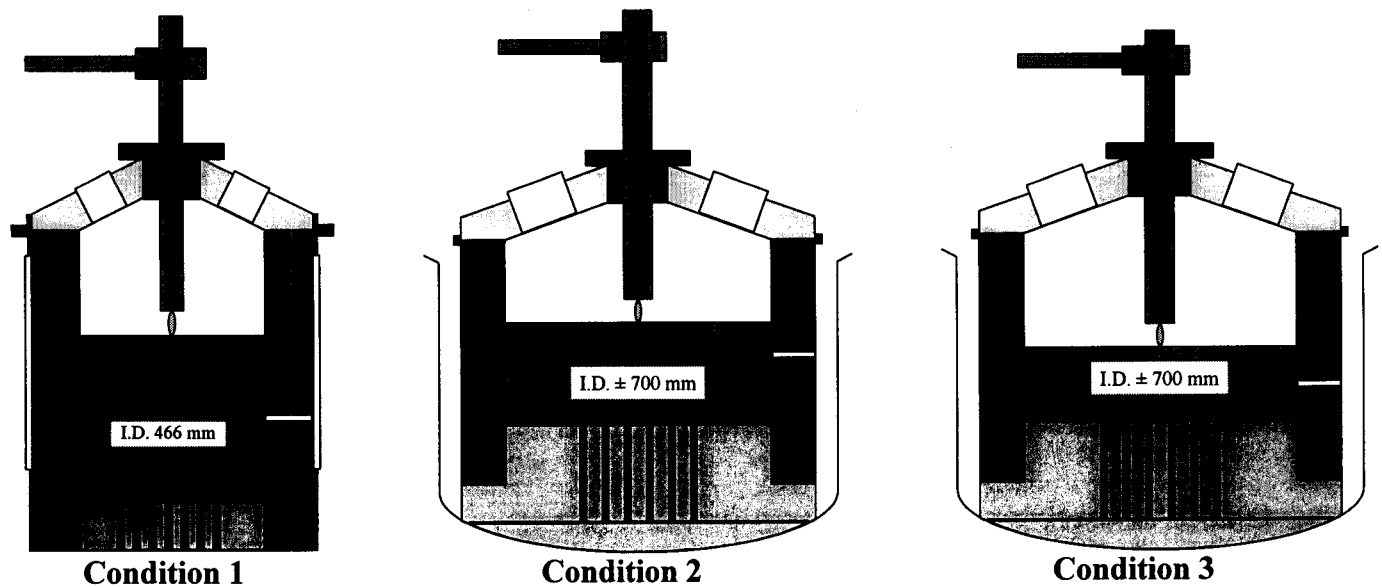

Condition 1   **Condition 2**   **Condition 3**

Figure 2 – Schematic diagrams of the two DC-arc furnaces, showing the different bath widths and depths tested

Furnace operation

Both furnaces were run from the same 200 kVA power supply. The important operating details (slightly simplified) are listed in Table I.

Table I – Operating details

Slag batch size	120 kg
Slag feed rate	60 kg/h
Coke batch size	4.8 kg
Energy requirement	0.6 kWh/kg slag
Temperature	1500°C
Power	36 kW + losses

Feed materials

The chemical analysis of the slag feed is shown in Table II, and the analysis of the coke (used as a reductant) is shown in Table III.

Table II – Composition of feed slag, mass %

	Al_2O_3	CaO	Co	Cr_2O_3	Cu	FeO	MgO	Ni	S	SiO_2	Total
Feed slag	1.72	1.17	0.19	0.20	0.07	31.2	18.1	0.24	0.53	44.1	97.0

Table III – Chemical analysis of coke, mass %

	Fixed C	Ash	Volatiles	Moisture	S	Total
Coke	76.8	17.3	5.1	0.2	0.6	100

	Al_2O_3	CaO	FeO	MgO	SiO_2	Total
Ash	19.66	3.07	11.86	1.04	60.67	96.3

Products

The masses and analyses of the slag tapped are presented in Table IV, along with the tapping temperatures. Weighted averages are shown for each condition.

Table IV – Mass and analysis (mass %) of slags tapped

Tap No.	Mass, kg	Co	Cu	Ni	S	Al_2O_3	CaO	Cr_2O_3	FeO	MgO	SiO_2	Total, %	T, °C
1.1	135.0	0.028	0.017	0.011	-	2.31	1.34	0.50	28.95	19.10	46.00	98.25	1453
1.2	117.0	0.019	0.014	0.007	0.22	2.15	1.40	0.34	24.31	20.70	49.60	98.54	1451
1.3	112.0	0.018	0.015	0.008	-	2.41	1.32	0.45	22.38	20.90	50.30	97.81	1505
1.4	111.5	0.017	0.014	0.006	0.21	2.41	1.37	0.52	21.74	21.00	50.90	97.98	-
1.5	117.0	0.023	0.017	0.014	-	2.27	1.47	0.55	22.77	20.50	49.60	97.21	-
1.6	101.5	0.022	0.017	0.050	-	2.28	1.37	0.52	21.87	20.90	52.30	99.33	-
Condition 1	**115.7**	**0.021**	**0.016**	**0.015**	**0.22**	**2.30**	**1.38**	**0.48**	**23.87**	**20.46**	**49.62**	**98.17**	**1468**
2.1	162.5	0.037	0.032	0.014	-	1.90	1.25	0.24	32.68	17.50	44.90	98.55	1521
2.2	158.5	0.034	0.027	0.012	0.28	1.94	1.28	0.22	29.33	17.90	48.20	98.94	1521
2.3	109.5	0.045	0.030	0.017	-	2.10	1.30	0.24	28.43	18.50	48.80	99.46	1486
2.4	117.0	0.032	0.026	0.010	-	2.12	1.29	0.25	27.53	18.80	47.75	97.81	1511
2.5	96.5	0.035	0.025	0.011	0.26	1.97	1.28	0.22	27.66	18.80	47.40	97.40	1458
2.6	102.5	0.029	0.023	0.010	-	2.05	1.35	0.23	25.73	19.20	49.90	98.52	1547
2.7	120.0	0.032	0.022	0.008	-	2.10	1.35	0.22	25.09	19.10	48.70	96.62	1526
2.8	114.0	0.032	0.023	0.011	0.24	2.22	1.37	0.23	24.83	19.30	49.90	97.92	1501
2.9	138.0	0.031	0.023	0.010	-	2.34	1.36	0.22	24.70	19.90	49.80	98.38	1510
2.10	199.0	0.031	0.023	0.008	-	2.12	1.33	0.24	24.96	19.50	50.30	98.51	1503
Condition 2	**131.8**	**0.034**	**0.025**	**0.011**	**0.26**	**2.08**	**1.31**	**0.23**	**27.18**	**18.83**	**48.55**	**98.27**	**1509**
3.1	97.5	0.045	0.028	0.019	-	2.10	1.28	0.22	26.12	19.00	48.70	97.51	1531
3.2	134.0	0.034	0.024	0.012	0.25	2.26	1.29	0.24	25.86	19.20	48.80	97.72	1526
3.3	120.0	0.040	0.025	0.021	-	2.13	1.31	0.27	24.70	19.70	49.50	97.70	1553
3.4	139.0	0.042	0.025	0.016	-	2.11	1.29	0.27	26.37	18.80	48.50	97.43	1537
3.5	95.0	0.045	0.026	0.016	0.27	2.10	1.24	0.26	27.14	18.40	48.85	98.08	1512
3.6	115.0	0.034	0.024	0.012	-	2.17	1.25	0.27	26.24	18.50	50.00	98.50	1545
3.7	115.0	0.043	0.027	0.015	-	2.14	1.31	0.26	27.53	18.40	47.80	97.53	1549
3.8	104.0	0.041	0.025	0.017	0.26	2.15	1.34	0.25	27.14	18.50	48.40	97.87	1509
3.9	117.0	0.032	0.023	0.009	-	2.13	1.31	0.26	27.14	18.70	48.10	97.71	1504
3.10	153.0	0.034	0.023	0.011	-	2.09	1.32	0.27	27.40	18.50	47.70	97.35	1509
Condition 3	**119.0**	**0.039**	**0.025**	**0.015**	**0.26**	**2.14**	**1.30**	**0.26**	**26.56**	**18.78**	**48.61**	**97.72**	**1528**

The most striking feature of the results is the clear difference in the cobalt content of the slag produced under the different conditions. The residual cobalt, nickel, copper, and FeO levels in the slag are shown graphically in Figure 3. The actual analyses are shown on a tap-by-tap basis, and the 95% confidence limits are superimposed on the graphs, clearly showing the distinct differences between the conditions. The confidence limits shown were calculated on the assumption of a normal distribution having the same calculated mean and standard deviation as the data points presented. No confidence intervals are shown for FeO, as the trend in these values is discussed later.
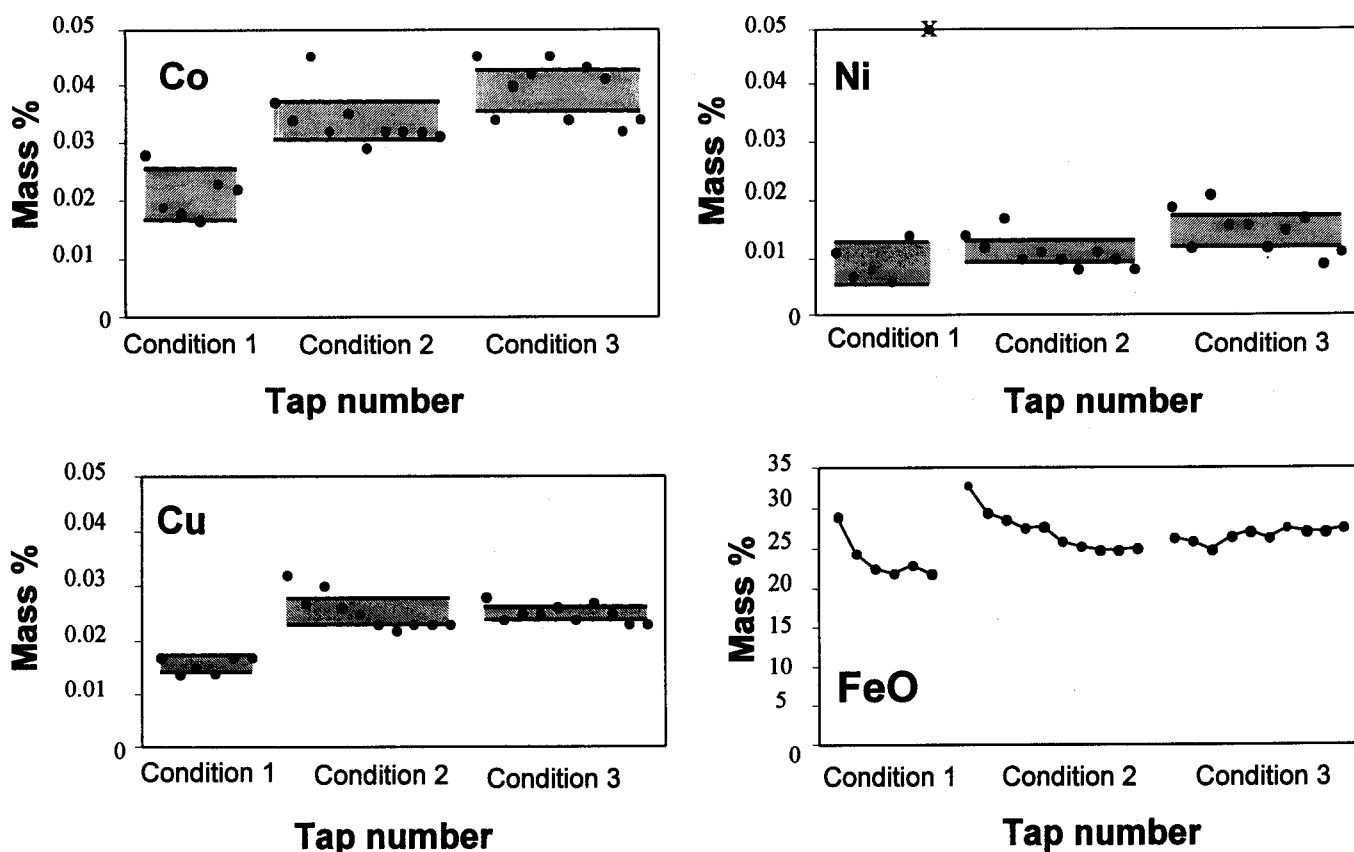
Figure 3 – Co, Ni, Cu, and FeO levels in the tapped slags (with 95% confidence levels)

The masses and analyses of the metal produced during the campaign are presented in Table V.

Table V – Mass and analysis of metal produced

Condition	Mass, kg	Co, %	Cu, %	Ni, %	Fe, %	S, %	Si, %	C, %	Total, %
1 (top)		7.47	3.91	20.3	64.2	3.1	-	0.02	99.0
1	153	2.99	1.07	6.18	86.8	1.1	-	0.04	98.2
2,3	180	2.18	0.74	3.77	84.4	5.8	0.16	0.04	97.1

The metal produced during Condition 1 does not really represent the composition of the metal that would be produced in industrial operation of this process, as it includes metal produced, at the end of a series of taps, from other higher-grade feed material (not reported on here) as well. The two metal samples were dug out of the furnace at the end of the furnace campaign. Because of some degree of contamination of the relatively small amounts of metal produced, by dilution with the metal heel of the furnace, the metal analyses may not be exactly representative of the large-scale operation of the process. As a far greater quantity of slag is produced than metal, it is better to calculate the expected metal analysis and quantity on the basis of the measured slag values.

During this campaign, the measured dust loss was 0.4 per cent of the mass of feed slag, although this result may have limited significance at the scale of operation used in these tests.

Accountability

Accountabilities were calculated for each of the important elements after completion of the furnace campaign. The final alloy produced was dug out of the furnace, and was very difficult to sample accurately because of its extreme toughness. The accountabilities (for the portion of the campaign using the larger furnace shell) were 104% for silicon, 105% for calcium, 101% for iron, 98% for cobalt, 107% for copper, and 114% for nickel. The consistent over-accounting for silica and lime indicates a probable small systematic error in the slag mass measurements. It is suspected that sampling errors with the alloy led to the over-accounted quantities of nickel and copper.

Simulation and mass-balance reconciliation

Prior to the furnace campaign, a predictive simulation (based on chemical equilibrium, calculated by free-energy minimization) was carried out, using Pyrosim computer software (2). The purpose of this simulation was to give some indication of the expected slag and metal masses and bulk compositions, as well as to determine the expected energy requirement (and reductant addition) for the process. The Ideal Mixing of Complex Components (IMCC) modelling approach was used to account for some of the non-ideal behaviour of the slag and alloy solution phases. The equilibrium simulation, at a temperature of 1500°C, assumes that all the coke fed is consumed by the reactions. Based on experience with similar processes, an entrainment of two per cent of the metal in the slag was assumed. Table VI compares the experimental results with the simulation, and also includes figures obtained from empirical simulations.

Table VI – Empirical simulated mass balances for each condition, with some experimental data

	Equilibrium	Condition 1		Condition 2		Condition 3	
	Equilib Sim.	Exp.1	Sim.1	Exp.2	Sim.2	Exp.3	Sim.3
Slag feed, kg	120.0	120.5	120.0	120.1	120.0	120.1	120.0
Coke feed, kg	4.8	4.6	4.8	4.6	4.8	4.8	4.8
Gas, kg	10		10		9		9
Slag, kg	103	116	104	132	109	119	108
Co, %	0.02	0.021	0.021	0.034	0.034	0.039	0.039
Cu, %	0.002	0.016	0.016	0.025	0.025	0.025	0.025
Ni, %	0.01	0.015	0.015	0.011	0.011	0.015	0.015
Al_2O_3, %	2.18	2.30	2.14	2.08	2.05	2.14	2.07
CaO, %	1.39	1.38	1.37	1.31	1.31	1.30	1.32
Cr_2O_3, %	0.23	0.48	0.23	0.23	0.22	0.26	0.22
FeO, %	23.0	23.87	23.87	27.18	27.18	26.56	26.56
MgO, %	21.2	20.5	20.8	18.8	19.9	18.8	20.1
SiO_2, %	52.1	49.6	51.3	48.6	49.0	48.6	49.4
S, %	0.02	0.22	0.22	0.26	0.26	0.26	0.26
Metal, kg	13		11	9.1	7.0	9.1	7.8
Co, %	1.69		1.91	2.2	2.71	2.2	2.40
Cu, %	0.66		0.62	0.74	0.81	0.74	0.74
Fe, %	86.7		90.9	84	87.1	84	88.4
Ni, %	2.25		2.52	3.8	3.92	3.8	3.51
S, %	8.67		4.02	5.8	5.42	5.8	4.95
kWh / kg of slag	0.73	0.64	0.74	0.72	0.72	0.74	0.72
Co recovery, %	93		90		84		81
Cu recovery, %	98		80		68		68
Fe recovery, %	37		34		21		23
Ni recovery, %	98		95		96		94

Note: Shaded figures are those specified in the empirical balance

In order to provide a self-consistent representation of the process mass balance, some empirical simulations were carried out using the Pyrobal model in the Pyrosim software package. For each condition, the experimentally-obtained average percentages of Co, Cu, Ni, FeO, and S, in the slag were specified (as these variables are believed to be known accurately). One further assumption (borne out by the results) is that effectively none of the sulphur reports to the gas phase. The remaining unknowns in the mass balance are calculated in terms of these specified variables. The empirically calculated mass balances provide an accurate representation of the conditions studied. A temperature of 1500°C was used for all simulations.

In the case of the empirical simulations, there is generally very good agreement between the simulated and experimental compositions. The differences between the experimental and simulated slag and metal masses can be explained, to a large degree, by the fact that the feed material fed during the warm-up period has not been included in the tap-to-tap averages shown in Table VI. The Cr_2O_3 value for Condition 1 is higher than that simulated because of the refractory wear in the furnace while operating at high power fluxes at this small scale.

Residence time

Mineralogical studies have shown that the cobalt in the slag is usually present in the oxide form, and is associated primarily with Fe_2SiO_4. Most of the nickel (and copper) is present as entrained metal or sulphide droplets. The cobalt oxide, and, to a lesser extent, the nickel and copper oxides associated with the silicate / oxide phases, is reduced by Fe from the alloy to form metallic Co (and Ni and Cu), resulting in the formation of FeO in the slag. Given that this reaction occurs between the metal and the slag, the exchange of Co with Fe will take place only at the slag/metal interface. Improved recoveries of valuable metals can be achieved by allowing greater quantities of slag to come into contact with the alloy (by mild stirring, for example), and increasing the length of the contact time between slag and metal.

Previous work (1) has shown the influence of retention time on the degree of cobalt extraction achieved in this process. In the previous tests, the furnace bath was allowed to stand and 'stew' for up to two hours after the full batch of slag had been fed. In the present work, the process was run on a more continuous basis, and the contents of the furnace bath were tapped out after each batch had been fed. However, it was still necessary to calculate a mean residence time, for the purposes of comparing the three conditions in the present test.

Assumptions

All three conditions were run at a relatively constant feed rate of about 60 kg of slag per hour. However, the quantity of slag remaining in the furnace after each tap differed for each condition. The material remaining in the furnace was essentially the portion of the molten bath below the level of the taphole. For the purposes of calculating a mean residence time to characterise each condition, it was assumed that the batch was fed perfectly evenly over the duration of each feeding period. The furnace contents at the beginning of a tap were level with the taphole, and increased linearly in height during the tap. Once the taphole was opened, the contents were drained down to the level of the taphole again. It is assumed that the furnace contents were perfectly mixed. It is clear that the mean residence time is increased by a larger volume of material retained in the furnace.

Calculation method

The method for calculating the mean residence time of a semi-continuous batch process is not standard textbook material, and so is briefly outlined here. It is possible to calculate the amount of feed from any particular tap number that is in the furnace at any given time, provided the amount of material lying below the taphole is known. Using the exact masses fed during the warm-up periods, the exact mass fed and tapped in the first tap and an average of the mass tapped in all later taps, it is possible to determine (with reasonable accuracy) how much material lies below the taphole. Then, using the exact masses for the warm-up stages and the first tap, and the average mass tapped as the input and exit mass for any further taps, the proportion of mass from each tap that is in the furnace can be found at any given time. Also, from the

actual tap-to-tap time, it is possible to obtain the mean residence time for each portion of feed in the furnace at a given time. Summing the product of the proportions of feed and the respective mean residence times gives the actual mean residence time for all material in the furnace at a particular time.

To illustrate the method of calculation more clearly, consider the following example, depicted in Figure 4. A set mass is fed into the furnace (at an assumed constant feed rate) over a 2-hour time period. This mass is considered to be the initial warm-up mass fed, i.e. no tapping occurs at the end of this stage. This mass has a mean residence time of 1 hour. The same set mass is again fed into the furnace (i.e. feed for tap 1), again at a constant feed rate, over 2 hours. Just before the furnace is tapped, the warm-up feed has a mean residence time of 3 hours, whilst the material fed during tap 1 has a mean residence time of 1 hour. However, since the amount from each feed was identical, the mean residence time of any random particle removed from the furnace is 2 hours. Now, when the same set mass is fed during tap 2, this mass forms half of the total mass in the furnace, and has a mean residence time of 1 hour just before tapping. Also, at this point, the warm-up feed constitutes one quarter of the total mass in the furnace (mean residence time 5 hours) and the feed from tap 1 forms the remaining quarter of the total furnace mass (mean residence time 3 hours). In this case, the mean residence time of any random particle removed from the furnace is 2.5 hours. Similarly, it is possible to calculate the mean residence time of any particle at any other point in time, and the calculations can be continued until steady state has been reached.

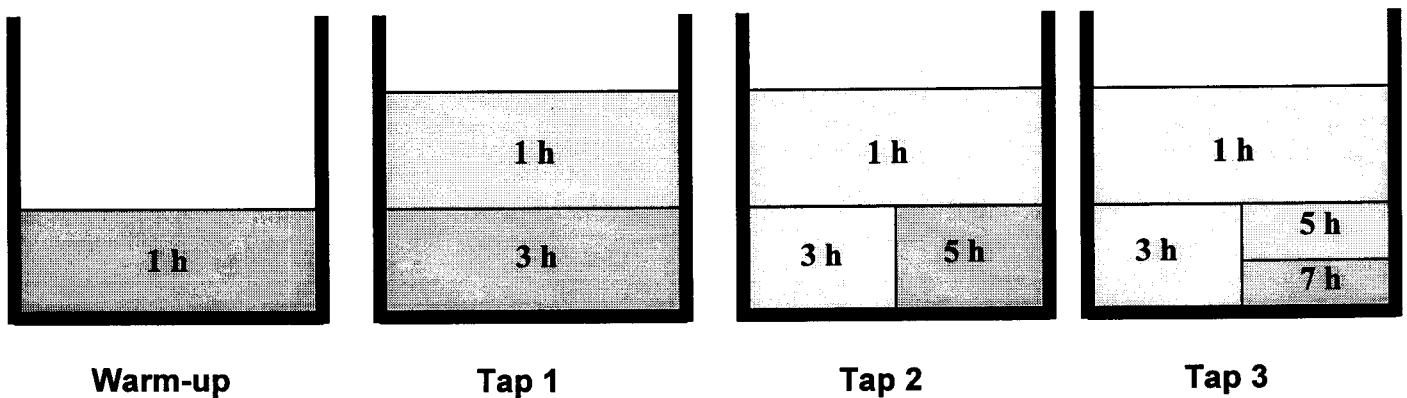**Warm-up**   **Tap 1**   **Tap 2**   **Tap 3**

Figure 4 – Example showing how mean residence times are calculated at the end of each tap

The tap-to-tap times and mean residence times for each tap are listed in Table VII.

Table VII – Tap-to-tap times and mean residence times for each tap

Condition 1	Warm-up	Tap 1.1	Tap 1.2	Tap 1.3	Tap 1.4	Tap 1.5	Tap 1.6
Time between taps, h	3.42	2.17	3.37	2.15	2.47	2.30	2.23
Feeding time, h	3.42	2.08	2.70	2.15	2.32	2.23	2.10
Mean residence time, h	1.71	2.52	3.69	3.53	3.65	3.61	3.52

Condition 2	Warm-up	Tap 2.1	Tap 2.2	Tap 2.3	Tap 2.4	Tap 2.5	Tap 2.6	Tap 2.7	Tap 2.8	Tap 2.9	Tap 2.10
Time between taps, h	5.33	2.17	2.78	2.17	2.30	2.12	2.12	2.17	2.63	2.35	2.60
Feeding time, h	4.82	2.12	2.62	2.08	2.25	2.08	2.12	2.12	2.37	2.23	2.42
Mean residence time, h	2.66	3.66	4.74	4.96	5.23	5.26	5.28	5.33	5.72	5.76	5.99

Condition 3	Tap 3.1	Tap 3.2	Tap 3.3	Tap 3.4	Tap 3.5	Tap 3.6	Tap 3.7	Tap 3.8	Tap 3.9	Tap 3.10
Time between taps, h	2.20	2.37	2.25	2.30	2.18	2.45	2.20	2.37	2.68	2.75
Feeding time, h	2.13	2.33	2.22	2.28	2.12	2.20	2.15	2.22	2.67	2.73
Mean residence time, h	4.64	4.09	3.73	3.59	3.42	3.49	3.39	3.44	3.73	3.93

It is interesting to note that an average tap-to-tap time of about two and a half hours can result in a mean residence time of up to six hours. This is influenced primarily by the fraction of material remaining in the furnace at the end of each tap, as well as by the duration of the warm-up period. (It is in fact possible to select a particular warm-up period that results in a constant mean residence time across all taps. This period would, of course, differ according to the fraction of material remaining in the furnace between taps. For example, for a tap-to-tap time of 2 hours, if half of the material remains in the furnace at the end of each tap, a warm-up period of 6 hours, with steady feeding, is required to ensure a constant mean residence time of 3 hours for all taps. Any warm-up period different from this would produce mean residence times that tended towards this same asymptotic value.) Of course, one should bear in mind that the mean residence time does not tell the whole story – the actual distribution of residence times also matters.

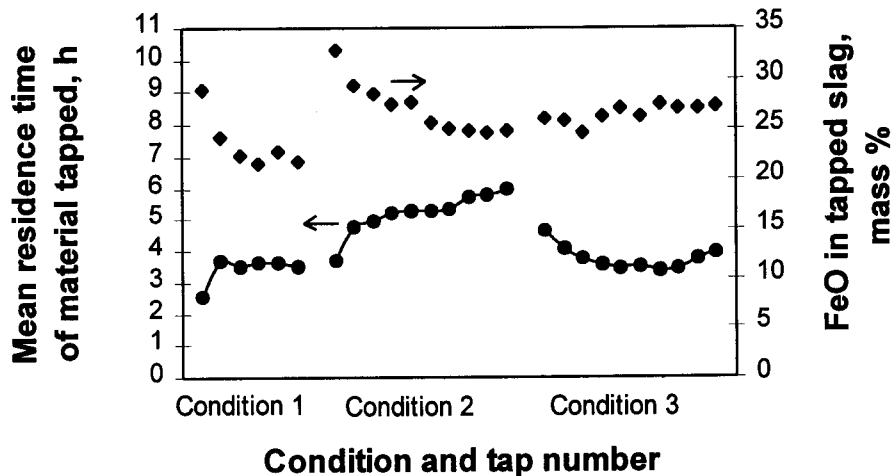The mean residence times are shown, together with FeO levels in the slag, in Figure 5.

Figure 5 – Mean residence time for each tap (as well as FeO in slag)

Figure 5 illustrates a distinct (inverse) correlation between the FeO remaining in the slag, and the mean residence time of the material tapped from the furnace. The change in pattern for the residence time distribution of Condition 3 (apart from the fluctuations in experimental conditions) can be ascribed to the fact that the operation simply continued (in the same furnace shell, using the lower taphole) from Condition 2 to Condition 3, albeit at a lower level of molten material in the furnace. This continuation of the operation implies that the material remaining in the furnace had a longer time available to approximately reach its 'steady-state' residence time distribution. The copper remaining in the slag shows an inverse variation with the mean residence time, similar to that shown by FeO, albeit less pronounced because of the low levels present. Somewhat surprisingly, there is not much of a direct correlation between the cobalt and nickel remaining in the slag (shown in Figure 3) and the mean residence time, on a tap-to-tap basis.

Electrical properties
The electrical characteristics of the bath and arc were measured under the various conditions of interest. The variables of temperature and chemical composition were assumed constant for our purposes. The bath resistance (Ω) was calculated by dividing the potential difference (V) across the bath by the current (A). These measurements were taken as close as possible to an arc length of zero, i.e. when the electrode tip just touched the surface of the bath. Measurements were taken for a number of taps, as there is a great deal of experimental scatter present. The value used for the bath resistance was the slope of the voltage versus current line, as there is expected to be some voltage drop across the interface between electrode and slag. As the molten bath is wider than the current path, the bath resistance may be assumed to be a function of depth only. The measured bath resistances are presented in Table VIII.

Table VIII – Bath resistance as a function of depth

Bath depth, cm	9	18	19	20	29	40
Bath resistance, Ω	0.03	0.04	0.04	0.04	0.05	0.06

Voltages and currents were also measured at a number of different arc lengths, and the arc voltage was calculated from the following relationship:

$$V_{arc} = V_{total} - I \times R_{bath}$$

Averaged over the entire campaign, the arc voltage may be expressed as a function of the arc length, as follows:

$$V_{arc} = 74\ V + 4.1\ V \text{ per cm of arc length}$$

It is of interest to know the ratio of the power dissipated in the arc to that dissipated in the molten bath. This may easily be calculated, using the total power, total voltage, and the calculated bath resistance. (As the same current passes through the arc and the bath, it is clear that the ratio of arc power to bath power is equal to the ratio of arc voltage to bath voltage.) The results of this calculation are shown in the overall comparison of the three conditions, in Table IX.

Overall comparison

In such a small number of tests, it is very difficult to isolate the effects on the process of changes in the many variables involved. (However, it is hoped that this work will stimulate the further investigation of some of the issues highlighted here.) Table IX compares the averaged furnace operating parameters for each condition.

Table IX – Comparison of furnace operating parameters, averaged over each condition

	Condition 1 Narrow, deep	Condition 2 Wide, deep	Condition 3 Wide, shallow
Width, m	0.466	0.700	0.700
Depth, m	0.400	0.280	0.190
Surface area, m^2	0.171	0.385	0.385
Bath volume, m^3	0.068	0.108	0.073
Power, kW	81	95	104
Power loss, kW	48	56	65
Useful power, kW	33	39	38
Power flux, kW/m^2	477	247	270
Temperature, °C	1468	1509	1528
Voltage, V	140	135	150
Current, A	580	700	690
Varc / Vtotal, %	75	74	82
Tap duration, h	2.53	2.32	2.35
Feed period, h	2.15	1.98	1.98
Residence time, h	3.39	5.18	3.75
Feed rate of slag, kg/h	56	61	61
Specific energy, kWh/kg of feed slag	0.64	0.72	0.74
Co in slag, mass %	0.021	0.034	0.039
Cu in slag, mass %	0.016	0.025	0.025
Ni in slag, mass %	0.015	0.011	0.015
FeO in slag, mass %	23.9	27.2	26.6
Co recovery, %	90	84	81
Cu recovery, %	80	68	68
Ni recovery, %	95	96	94

The electrode consumption over this campaign was 1.6 kg/MWh, or 3.2 kg/t slag fed.

There is a marked difference between the results obtained under the three conditions, with cobalt recovery to the metal varying between 81 and 90%, and nickel recovery varying between 94 and 96%. Copper recovery varied between 68 and 80%.

As bath depth increases, so cobalt extraction improves. (Together with the best cobalt recovery goes the highest iron content in the alloy.) Condition 1 shows a marked increase in cobalt recovery over the two other conditions. Condition 2 has a larger slag / metal interfacial area potentially available for mass transfer, yet even this was not enough to offset the benefits of the deeper bath in Condition 1. The reasons for this apparent behaviour are not altogether clear. Perhaps the increased stirring arising from the higher power fluxes played a part.

The nickel results need to be interpreted carefully, as the nickel content in the slag for Condition 1, shown in Figure 3, has one outlying value (for tap 1.6) that raises the average used for the calculation of recoveries. Excluding this value would result in an average nickel content in the slag of 0.009% for Condition 1, which is the lowest over all the conditions. Overall, the best average nickel recovery is achieved under conditions of maximum bath volume and maximum mean residence time (which can be accomplished without increasing the tap-to-tap time, merely by increasing the fraction of molten material remaining in the furnace after tapping).

Copper recovery varied between 68 and 80%, with the best results being obtained under conditions of greatest bath depth and power flux (Condition 1).

CONCLUSIONS

There is a significant difference in residual cobalt and nickel levels between DC-arc furnace slag-cleaning processes run at different bath depths and heights. Power flux and mean residence time are directly affected by the furnace geometry. Furnace bath geometry plays a very important role in optimizing the efficiency of the process. Further work is required, under a different set of conditions (preferably at larger scale), in order to build on the results presented here, and to establish how the findings of the present work can be applied to a wider range of furnace sizes.

- Cobalt recovery varied between 81 and 90 per cent, depending on the furnace geometry. Cobalt recovery was maximized in a deep bath.

- Nickel recovery varied between 94 and 96 per cent, and was maximized by having a bath of large volume, and by increasing the mean residence time.

- Iron reduction was shown to vary with the mean residence time in the furnace, for a given furnace geometry.

- The mean residence time in the furnace can be increased without having to increase the tap-to-tap time, by simply increasing the fraction of molten material remaining in the furnace after tapping.

ACKNOWLEDGMENTS

REFERENCES

1. R.T. Jones, D.A. Hayman, and G.M. Denton, "Recovery of cobalt, nickel, and copper from slags, using DC-arc furnace technology", <u>International Symposium on Challenges of Process Intensification, 35th Annual Conference of Metallurgists</u>, CIM, Montreal, Canada, 24-29 August 1996, 451-466. http://www.mintek.ac.za/Pyromet/Cobalt.htm

2. R.T. Jones, "Computer Simulation of Pyrometallurgical Processes", <u>APCOM 87, Proceedings of the Twentieth International Symposium on the Application of Mathematics and Computers in the Minerals Industries</u>, Volume 2: Metallurgy, SAIMM, Johannesburg, October 1987, 265-279. http://www.mintek.ac.za/Pyromet/Pyrosim.htm

3. R.T. Jones, N.A. Barcza, and T.R. Curr, "Plasma Developments in Africa", <u>Second International Plasma Symposium: World progress in plasma applications</u>, EPRI (Electric Power Research Institute) CMP (Center for Materials Production), Palo Alto, California, 9-11 February 1993. http://www.mintek.ac.za/Pyromet/Plasma.htm